International Journal of Engineering Trends and Technology
ISSN: 2231–5381 / https://doi.org/10.14445/22315381/IJETT-V71I8P217

Volume 71 Issue 8, 191-200, August 2023

Original Article

Optimization of Flywheel for Reciprocating Air Compressor using Mayfly Algorithm

Atharva Barhanpurkar[1*], Deepak Hujare[1], Omkar Kulkarni[1], Abhijeet Birari[2]

[1]*Mechanical Engineering, MIT-WPU School of Mechanical Engineering, Maharashtra, India.*
[2]*R&D, Kirloskar Pneumatic Company Limited, Maharashtra, India.*

[*]*Corresponding Author : atharvabarhanpurkar@gmail.com*

Received: 27 March 2023 Revised: 18 June 2023 Accepted: 05 August 2023 Published: 15 August 2023

Abstract *- Reciprocating Compressors are typically used for low flow rates and high pressures. They are frequently used in mining and other sectors of the pneumatic industry. Flywheel pulleys are one of the key components used in compressors, among many other parts. The method uses a flywheel to buffer energy fluctuations, and a pulley transmits power effectively while slowing down the transmission. During this research, the flywheel's mass is optimized while keeping the moment of inertia the same as that of the old flywheel based on the compressor's requirement. Optimization, also referred to as mathematical programming, is a group of mathematical ideas and strategies for resolving quantitative issues in a variety of fields, such as physics, biology, engineering, economics, and business. A group of novel problem-solving methodologies and approaches that are inspired by natural processes are known as "nature-inspired algorithms". The flywheel optimization is carried out using a mayfly algorithm to cut down on material and production costs. The stressed-out model is validated using Ansys Mechanical. A mass reduction of 30% is obtained from this research.*

Keywords *- Flywheel pulley, Finite element analysis, Mayfly algorithm, Optimization, Reciprocating compressor.*

1. Introduction

Moving high-pressure air and gas for storage and use in a variety of applications is the main function of reciprocating compressors, also known as piston compressors. The main parts of the compressor are one or more cylinders and the pistons that move inside them. Similar to reciprocating compressors, automobile engines work by introducing air into one chamber, mixing it with fuel, and then forcing it under pressure out of a second chamber. The oil and gas sectors account for the bulk of reciprocating compressor uses. Oil refineries use these compressors for procedures that require high-pressure supplies of vital gases. In addition to natural gas transportation over pipelines, reciprocal compressors are also used.

Pulses, or areas of high and low pressure in relation to a constant pressure level, move through the pipe system as a result of a piston's reciprocating motion. It is possible to comprehend how pulsations are created by using a straightforward compressor piston without any valves. The piston's back-and-forth motion creates regions of compression and rarefaction, and they move through the piping system at the gas's sound speed. Pressure pulsations, or variations in pressure, are brought on by the positive and negative pressure areas moving away from the piston. These pulsations cause a very high load on the crankshaft. Also, due to the pressure variation, the energy requirement to drive the compressor varies continuously. In order to provide this fluctuating energy, flywheels are commonly used by industries.

Energy is stored in a flywheel. However, their primary function in machine design is to smooth out changes in shaft speed brought on by loads or power sources that fluctuate in a cyclical manner. A flywheel evens out the varying speed of a machine. It lessens unwelcome transient loads by using its kinetic energy of $0.5I\omega 2$ to absorb the change in torque during a machine cycle. Supplying energy at rates greater than the source, smoothing the output of reciprocating engines, and adjusting the orientation of mechanical systems using gyroscopes and reaction wheels, among other things, is the predominant application of the flywheel. Flywheels are normally built of steel and rotate on traditional bearings, typically only capable of a few thousand revolutions per minute.

The current flywheel utilized in the compressor weighs 265 kilograms and has a moment of inertia of 24.101 kilograms per square meter. The flywheel's high weight raises the price of production. The study's primary goal was to lower the cost of making flywheels by applying the mayfly optimization algorithm to lighten the material weight.

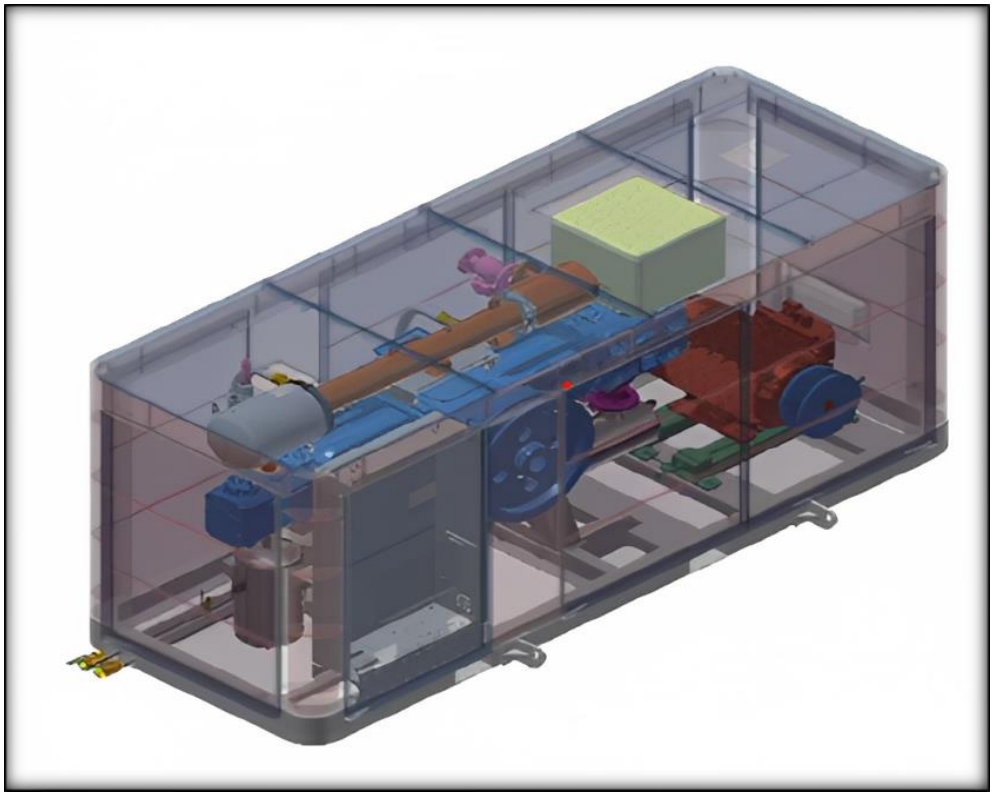

Fig. 1 Skid mounted reciprocating air compressor[1]

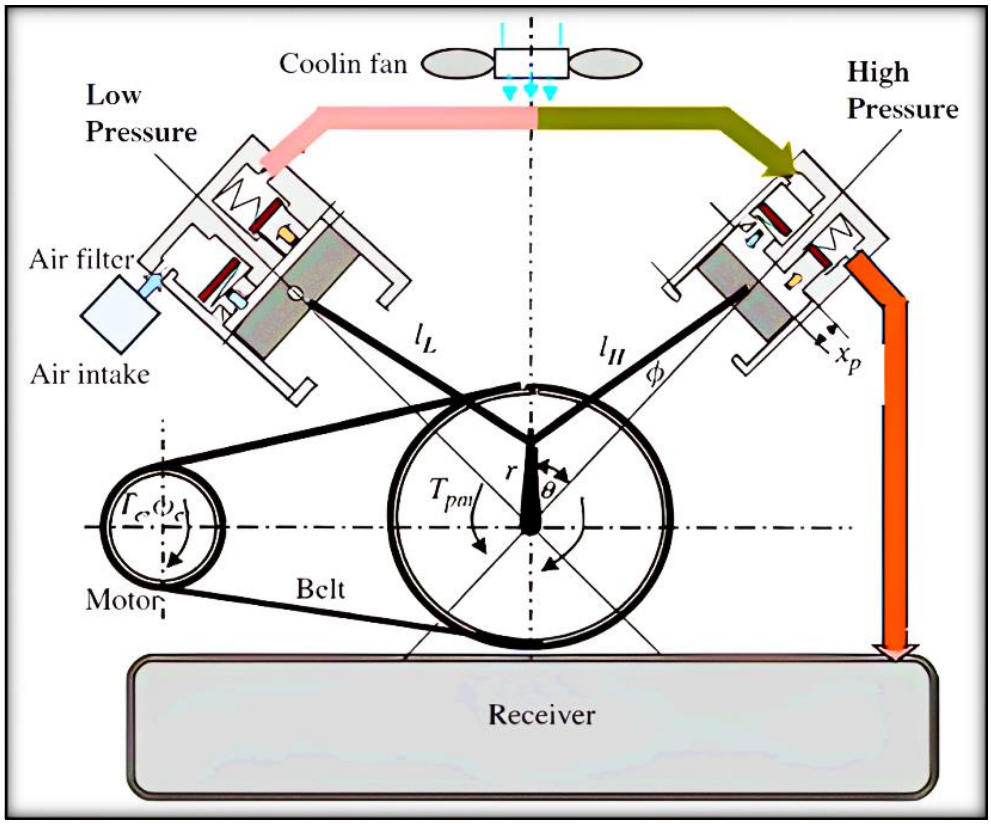

Fig. 2 Schematic and models of a two-stage compressor[2]

The term "nature-inspired optimization algorithms" (NIOAs) refers to a class of algorithms that draw their inspiration from natural phenomena, such as biological systems, swarm intelligence, physical and chemical systems, etc. Numerous popular NIOAs have been proposed thus far, including the genetic algorithm (GA)[3], particle swarm optimization (PSO)[4], differential evolution (DE)[5], artificial bee colony (ABC)[6], ant colony optimization (ACO)[7], cuckoo search (CS)[8], bat algorithm (BA)[9], firefly algorithm (FA)[26], grey wolf optimization (GWO)[11].

The flywheel was designed for a reciprocating compressor in the paper by considering the energy fluctuations required to drive the compressor. The moment of inertia required by the flywheel was calculated based on these fluctuations. For this moment of inertia, a new flywheel of optimum weight was designed using the mayfly algorithm. The shape of the flywheel was changed for optimization[12]. The results of the new optimized geometry were compared to the results of the existing flywheel. A conclusion was made that even though there is a slight increase in stresses, the flywheel is safe for operation as the total stresses of the final geometry are less than the allowable limit.

Singh and Chaudhary [13] developed a non-dominating Jaya algorithm for the optimization of the agricultural thresher flywheel. To generate a new design of the flywheel with the consideration of the multi-objective problem of kinetic energy and von-misses stresses. To plot the design variable points, a cubic B-spline curve is used. The proposed method is compared with the genetic algorithm. The results obtained that their algorithm results are much better than a genetic algorithm. After that, for validation purposes, the Ansys software is used for von-misses stresses. Fawazi and Hasrizam [14], in this study, used finite element analysis to forecast the flywheel's equivalent stress at various rotating speeds. Following the decision to set the maximum spinning speed at 8000 revolutions per minute, the flywheel's structure was modified. The maximal equivalent stress and the mass of the flywheel are both reduced as a result. This piece shows a contrast between the original and revised flywheel configurations. Gao and Zhao [15], with improved hybridization of the differential evolution (DE) and particle swarm optimization (PSO) methods, we present a novel technique for optimization termed the MO algorithm. In this study, they updated a velocity equation to the best of their ability. Simulation results demonstrated that the modified MO algorithm would outperform the baseline approach. Jiang & Wu [16] worked on flywheel performance as one of the key concerns to maximize energy storage density. The flywheel is subjected to topology optimization using the two-dimensional density approach. The improved flywheel topology arrangement was created using post-processing in conjunction with the finite element study that was performed. These topology-optimized flywheels can offer helpful recommendations for the design of energy storage flywheels in actual engineering. L Pedrolli and A Zanfei [17] worked on the optimization of energy-stored flywheels. They used a novel optimization approach for optimization. Utilizing an evolutionary system approach, the population's genome is optimised using statistical quantities. A complete description of the fitness function enables a wide range of goals. Jiang et al.[27]**,** presented a research study on the optimization of the flywheel rotor's form for energy storage. In which they developed a flywheel optimization method and parametric geometry model. In his research, it was discovered that form optimization is significantly impacted by the maximum structural stress constraint applied in the proposed region**.**

2. Methodology

A skid-mounted water-cooled reciprocating air compressor[1], as shown in Fig.(1), with a working pressure of 7.5 kg/cm2, was used for the study. The calculations in the further part of the study are based on the same. The schematic representation of a belt-driven reciprocating compressor for any general purpose is represented in fig.(2).

2.1. Compressor Calculations

A flywheel of a skid-mounted reciprocating air compressor is selected with a discharge pressure of 7.5 Kg/cm^2 and with a motor of 90 kW rating. The selected compressor is a double-acting type with two stages, increasing forces' action on the crankshaft. The forces acting on the crankshaft are calculated based on pressure variation during one compressor cycle.[20]

The force acting on the piston on the head end and crank end of the compressor is based on the difference between the suction pressure and the pressure at a particular instance of the stroke of the compressor is represented by eqn. (1)&(2).

$$F_{GH} = \frac{\pi}{4} D^2 (P_{HE} - P_S) \tag{1}$$

$$F_{GC} = (P_{HE} - P_S) A_{CE} \tag{2}$$

The total gas force acting on the piston is the sum of the gas force on the head end and crank end of the particular stage given by eqn. (3).

$$F_{GT} = F_{GH} + F_{GC} \tag{3}$$

The inertia force due to the mass of the piston and rotation of the crankshaft is given by eqn. (4)

$$F_I = \omega^2 \frac{M_r}{981} \left(\frac{cos(\theta) + cos2(\theta)}{n} \right) \tag{4}$$

The total force acting on the piston is given by the sum of the total gas force and the inertia force, as shown in eqn(5)

$$F_{Total} = F_{GH} + F_{GC} + F_I \quad (5)$$

The force required to drive the piston to resist the total force acting on it is given by eqn. (6)

$$F_{conrad} = \frac{F_{Total}}{cos(\emptyset)} \quad (6)$$

The force in the normal direction of the connecting rod is given by eqn. (7)

$$F_{Normal} = F_{conrad} sin(\emptyset) \quad (7)$$

This force is required on the crankshaft in the radial and tangential direction is represented by eqn(8)&(9).

$$F_{rad} = F_{conrad} cos(\theta + \emptyset) \quad (8)$$

$$F_{tangential} = F_{conrad} sin(\theta + \emptyset) \quad (9)$$

The torque required to provide the force from eqn.(9) is given by eqn.(10)

$$\tau = F_{tangential} \times r \quad (10)$$

Based on eqn. (10) the plot of torque for one rotation of the crankshaft is represented by fig.3

This is the torque needed to drive the crankshaft for the two-stage compressor. The variation in the torque requirement causes fluctuation in the energy needed to drive the compressor. This fluctuation can damage the motor that is used as the driver. So a flywheel is used as a buffer between the motor and compressor. Further, to reduce the overall cost of the compressor package, the flywheel is also used as a pulley that connects the compressor to the motor using a belt drive. The energy variation of the compressor was plotted based on the torque variation. This torque variation was put into the AutoCAD software to determine the area of the graph, and based on this area, the energy variation can be determined.

As shown in Fig.(4), the area of each region in mm^2, shaded with different color, is given in Table 1. By multiplying the value in column 3 of Table 1, we get the energy value in that particular region by scaling factor.

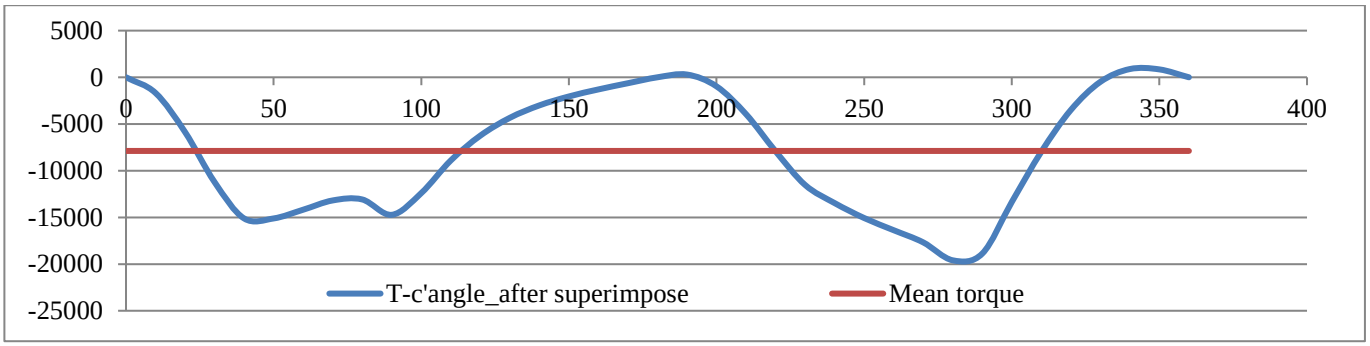

Fig. 3 Torque vs Theta diagram for compressor

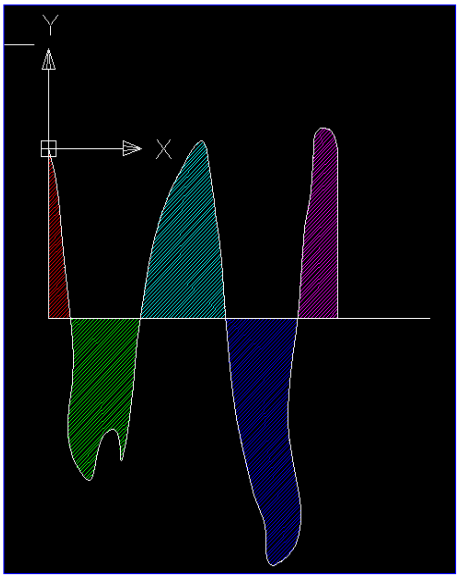

Fig. 4 Torque vs Theta diagram for energy calculation

Table 1. Energy of fluctuation during the cycle

Area Section	Hatch Section Color	Area Value (mm^2)	Area Value (N.M)
A1	Red	3158.78	270.41787
A2	Green	12297.96	1052.8078
A3	Cyan	14458.75	1237.7894
A4	Blue	17633.23	1509.5513
A5	Magenta	8502.57	727.8908

Table 2. Energy at points intersecting the mean line

Locations	Energy at 5 meeting points
a	270.4178727
b	-782.3899145
c	455.3994907
d	-1054.151838
e	-326.2610409

By cumulative addition of energies in each region, the fluctuation energy of that region can be determined, as shown in Table 2. This represents the energy of fluctuation of the compressor when the mean torque is acting.

The flywheel needs to compensate for the maximum variation in the energy requirement of the compressor. This can be determined by taking the difference between maximum and minimum energy values from Table 2. This is represented by eqn. (11)

$$\Delta E = E_{max} - E_{min} \quad (11)$$

$$\therefore \Delta E = 1509.5513$$

The maximum energy absorbed by a flywheel is given by eqn. (12)The compressor's operation speed is 754 rpm. Also, for a belt-driven flywheel pulley, the coefficient of fluctuation C_s is taken to be 1/80[22].

$$\Delta E = I.\omega^2 C_s \quad (12)$$

Form this eqn. (11), The minimum moment of inertia required for the flywheel can be calculated which is given by

$$\therefore I = 19.37\ kg - m^2 \quad (13)$$

2.2. Material of Flywheel

A flywheel needs to store maximum energy in minimum volume; the material density must be as high as possible. It is also desirable that the flywheel can be easily machined. The cost of material and machining cost of the flywheel must also be low so that it is feasible to manufacture and use in the package as such cast iron and cast steel are used. When the speed of flywheel operation is less than or equal to 40m/s, cast iron is used, and if the speed is more than 40m/s, cast steel is used. Also, as reciprocating compressor components undergo immense loads due to reciprocating action, a high factor of safety of order of 9 is considered [22].

For this work, a cast iron flywheel is considered. The material properties of cast iron and allowable stress values are given in Table 3.

Table 3. Material of flywheel[20]

Material	Cast Iron	**Units**
Density	7200	Kg/m^3
Young's Modulus	429	GPa
Tensile strength	260	MPa
Allowable strength	28.89	MPa

2.3. Mass Moment of Inertia and Mass of the Flywheel

Based on the geometry of the existing flywheel, as shown in fig.(5), the dimensions of different features are represented in Table 4.

Table 4. Existing flywheel dimensions

Sr. No.	**Description**	**Symbol**	**Value**	**Unit**
1	Material of flywheel	Cast Iron	7200	kg/m^3
2	Rim outer diameter	D_R	0.7600	Mtr.
3	Rim inner diameter	D_r	0.6060	Mtr.
4	Hub outer diameter	D_H	0.2075	Mtr.
5	Hub inner diameter	D_h	0.1080	Mtr.
6	Hole diameter	D	0.100	Mtr.
7	Hole PCD	PCD	0.3700	Mtr.
8	No. of holes	N	4	
9	Hub length	L_H	0.150	Mtr.
10	Rim length	L_R	0.150	Mtr.
11	Web thickness	T_W	0.045	Mtr.

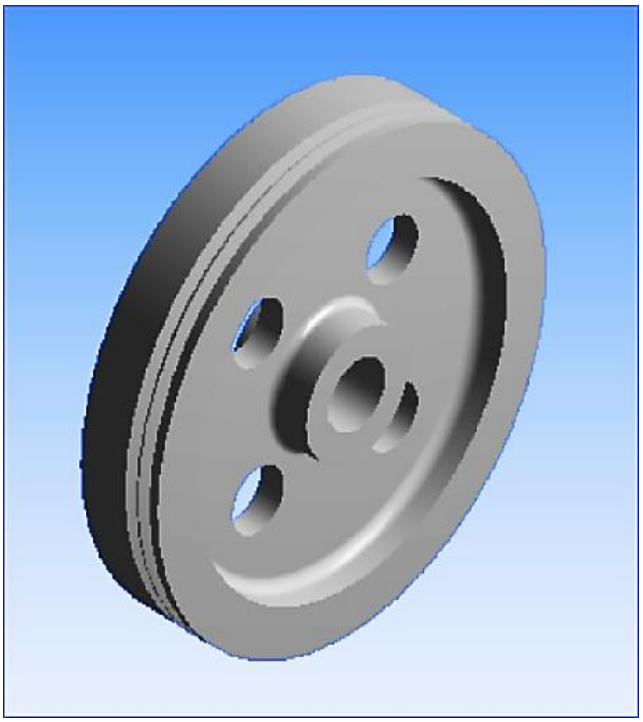

Fig. 5 Torque vs Theta diagram for compressor

The mass and moment of inertia of the existing flywheel are obtained from these dimensions, as shown in Tables 5 and 6, respectively.

Table 5. Mass moment of inertia of the flywheel

Sr. No.	**Description**	**Symbol**	**Value**	**Unit**
1	Rim	I_R	21.074	kgm^2
2	Hub	I_H	0.182	kgm^2
3	Web	I_W	3.205	kgm^2
4	Holes	I_h	0.090	kgm^2
Total mass moment of inertia I_T =			**24.101**	kgm^2

Table 6. Mass of flywheel

Sr. No.	Description	Symbol	Value	Unit
1	Rim	mR	158.437	kg
2	Hub	mH	26.628	kg
3	Web	mW	70.564	kg
4	Holes	mh	10.179	kg
5	Ring	mRg	0.000	kg
Total mass of flywheel Tm =			**265.808**	kg

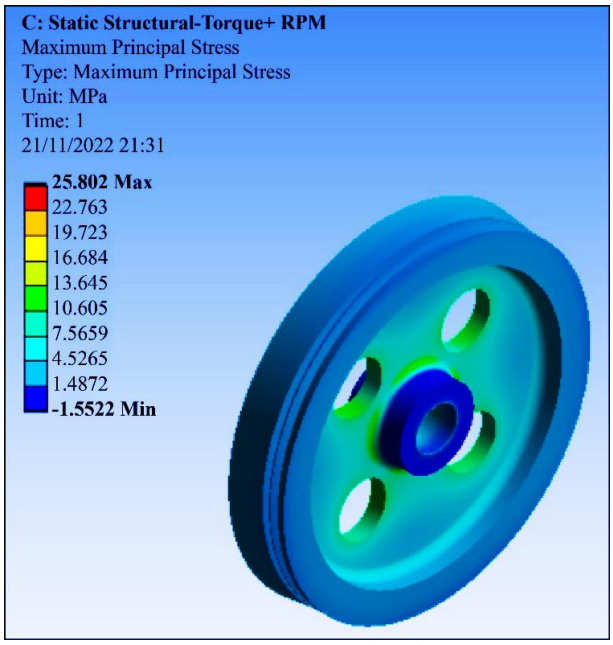

Fig. 6 Stress contour plot of the flywheel

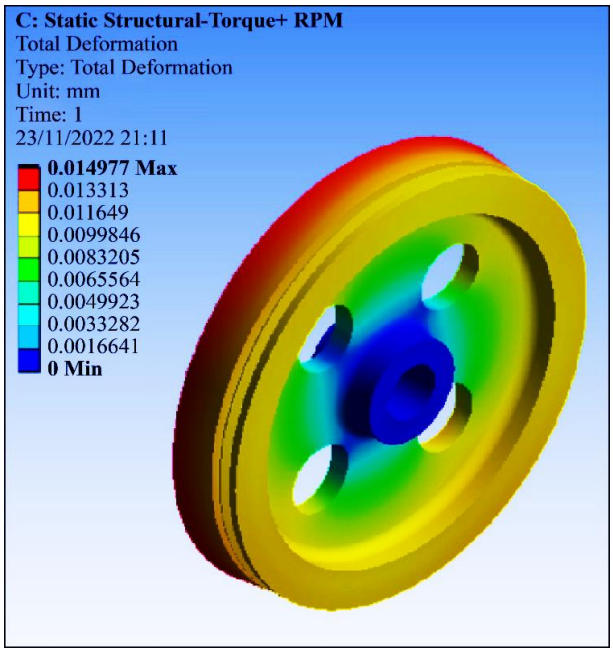

Fig. 7 Total deformation contour plot of the flywheel

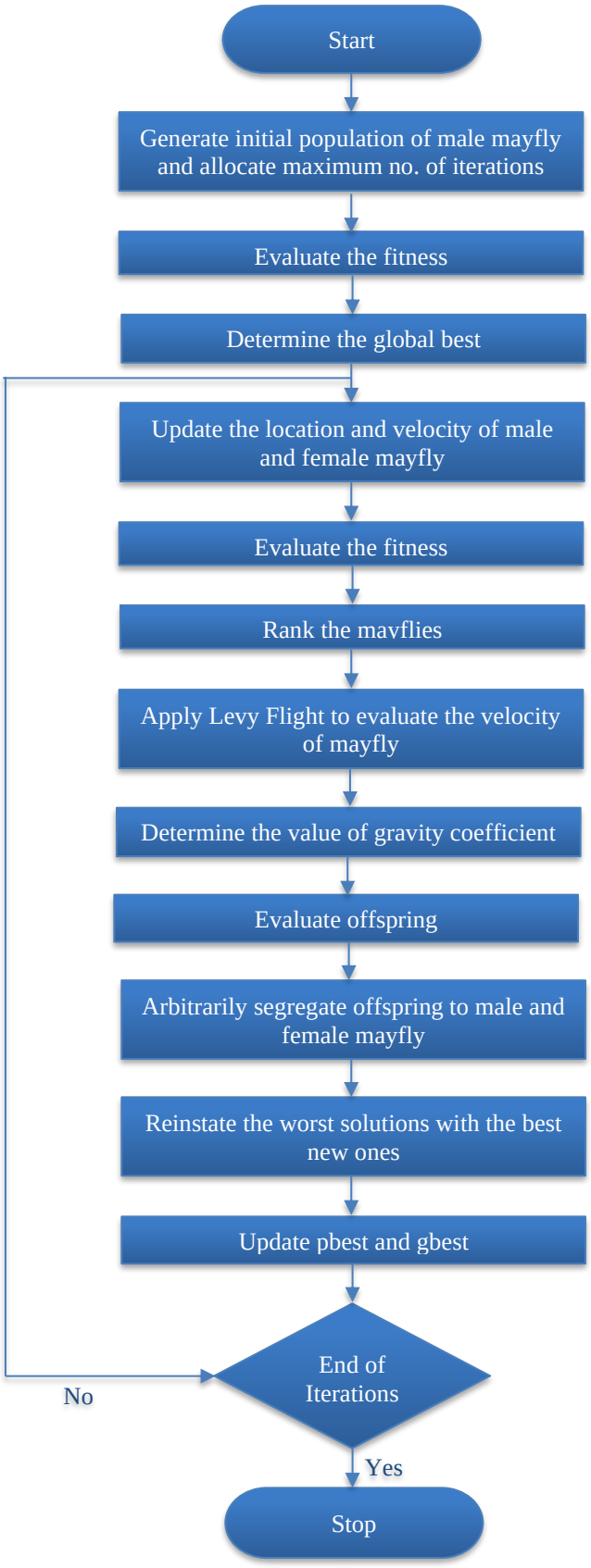

Fig. 8 Flowchart for mayfly algorithm [24]

After analyzing the existing flywheel from Table 5, it is observed that the moment of inertia is high. Thus the mass of the resulting flywheel also increases, as seen in Table 6. FEA analysis [21] was conducted on the flywheel, and loads due to centrifugal action and the belt tension are applied as shown. The allowable stress for Cast Iron was determined based on the factor of safety taken as 9, which came at 28.89MPa.

As can be seen from fig.6, there is a gradual change in stress distribution, with the minimum stress in the hub region, while the maximum stress is near the holes provided on the flywheel. The value of this stress is less than the allowable limit. Also, the total deformation in the flywheel, which is 0.015mm, is at the periphery of the rim, as shown in fig.7.

2.4. Optimization of the Flywheel

As the stresses are low, optimization was carried out to reduce the weight of the flywheel. Also, due to very low stresses, an arm type of flywheel was used instead of the solid rim-type flywheel. Using an AI-based optimization algorithm, determined the optimum dimensions of the flywheel. There are a lot of optimization algorithms which are based on the behavior of different animals and plants in nature. These algorithms take into account the methods in which the animal behaves to a particular change in nature, and based on that pattern, the algorithms are generated.

Mayfly Algorithm (MA) to solve optimization problems is inspired by the flight behavior and mating process of mayflies, and the algorithm combines major advantages of swarm intelligence and evolutionary algorithms. The order Ephemeroptera, which includes mayflies, is a suborder of the venerable Palaeoptera family of insects. Their name comes from the fact that May is when they are most prevalent in the UK. After emerging from the egg, immature mayflies can be seen with the naked eye. They spend several years developing as aquatic nymphs before they are ready to rise to the surface as adults.

The comparison's findings demonstrate that the suggested strategy is superior in terms of convergence rate and convergence speed. The mayfly algorithm may be implemented in any computer language, but we picked Matlab since it makes it simple to use structure arrays and create data visualisations. [23]

The total mass of the flywheel is the sum of the mass of the hub rim and the spokes combined, which can be represented by the following equation (14).

$$M = M_{hub} + M_{spoke} + M_{rim} \tag{14}$$

where, The eqn. (14) is the sum of eqn (15), (16) & (17)

$$M_{hub} = \rho \frac{\pi}{4}(d_o^2 - d_i^2)T \tag{15}$$

$$M_{spoke} = \rho bh \frac{(D_i - d_o)}{2} \tag{16}$$

$$M_{rim} = \rho \frac{\pi}{4}(D_o^2 - D_i^2)T \tag{17}$$

This mass needs to be minimized to reduce the cost of the flywheel and the overall cost of the compressor package. Also, the moment of inertia of the whole package must remain constant as given in eqn.13. As the flywheel is also used as a pulley and slots for belt mountings need to be provided, it reduces the moment of inertia of the flywheel, the design needs to consider some excess inertia as given in table 4. For arm type flywheel, the moment of inertia can be considered as the sum of the moment of inertia of the hub, rim and spokes about the centre of the hub, which is given as the sum of eqn(19),(20)&(21) and represented by eqn(18).

$$I = I_{hub} + N \times I_{spoke} + I_{rim} \tag{18}$$

where,

$$I_{spoke} = \frac{1}{8} M_{hub}(d_o^2 + d_i^2) \tag{19}$$

$$I_{spoke} = \frac{1}{3} M_{spoke} \left[\frac{(D_i - d_o)^2}{4} + \frac{b^2}{4} + \frac{d_o}{D_i}\left(\frac{3}{4}(D_i - d_o)^2 + \frac{3}{4}(D_i - d_o)d_o + \frac{1}{2}b^2 \right) \right] \tag{20}$$

$$I_{rim} = \frac{1}{8} M_{rim}(D_0^2 - D_i^2) \tag{21}$$

The optimization algorithm used helps to minimize the weight of the flywheel while providing the minimum moment of inertia. Also, the stresses in the flywheel must[25] be less than the allowable limit of 28.89 MPa.

2.4.1. Stresses in Rim

The stresses in the rim are given by eqn.(22) which can be obtained by solving eqn(23),(24),(25)&(26).

$$\sigma_{rim} = \rho r_a^2 \omega^2 \left[1 - \frac{f_4}{3} + \frac{A r_a}{3 Z_r}\left(f_4 - \frac{1}{f_3 \alpha} \right) \right] \tag{22}$$

$$f_1 = \frac{1}{2 sin^2(\alpha)}\left(\frac{sin 2\alpha}{4} + \frac{\alpha}{2} \right) \tag{23}$$

$$f_2 = f_1 - \frac{1}{2\alpha} \tag{24}$$

$$f_3 = \frac{A r_a^2 f_2}{J} + f_1 + \frac{A}{A_s} \tag{25}$$

$$f_4 = \frac{cos\beta}{f_3 sin\alpha} \quad (26)$$

2.4.2. Stresses in Spokes

Similarly, the stresses in the spoke can be calculated by taking the sum of bending(eqn(27)) and tangential stresses(eqn(28)) as shown in eqn(29).

$$\sigma_{b_{spoke}} = \frac{t(r_a - r_h)}{Z_s N_s r_a} \quad (27)$$

$$\sigma_{t_{spoke}} = \frac{\rho r_a^2 \omega^2}{6}\left(3 + \frac{4A}{f_3 A_s} - \frac{3r^2}{r_a^2}\right) \quad (28)$$

$$\sigma_{spoke} = \sigma_{t_{spoke}} + \sigma_{b_{spoke}} \quad (29)$$

If the flywheel is used as a pulley, the stresses acting are not evenly distributed, and as such, the number of spokes is divided by two during stress calculations.[25] Based on the above equations, the optimization problem is formulated, and the limiting values for different dimensions of the flywheel are

$$d_i = 0.11m$$
$$d_o = 0.20m$$
$$D_o = 0.76m$$
$$N = 6$$

Table. 7 List of variable parameters of the flywheel

Dimension	Representation	Min	Max
T	x_1	0	0.15
b	x_2	0	0.08
h	x_3	0	0.05
D_i	x_4	0.2	0.7

3. Results and Discussion

After using the mayfly optimization algorithm, the variable parameters were obtained in Table 8.

Table. 8 Output from the mayfly algorithm

Parameter	Representation	Value
Hub inside diameter	di	0.11m
Hub outside diameter	do	0.2m
Thickness of hub and rim	T	0.15m
Rim inside diameter	Di	0.641m
Rim outside diameter	Do	0.76m
Width of spoke	b	0.08m
Breadth of spoke	h	0.05m
Number of spokes	N	6

The new geometry was modelled after optimizing the flywheel using the mayfly algorithm. Fillets were added to reduce the stress concentration in the final model. The final 3D model for the flywheel with spokes is represented in fig.9.

The mass of the new geometry was found to be 199.22Kg by the modelling software after the material properties were applied.

Also, the moment of inertia for the new flywheel can be given by equation (18).

$$I = 23.982 \text{ kg} - \text{m}^2$$

So the moment of inertia of the new flywheel is almost the same as that of an existing flywheel. Ansys obtain the stress and deformation in the new geometry of flywheels.

Fig. 9 Optimized flywheel geometry

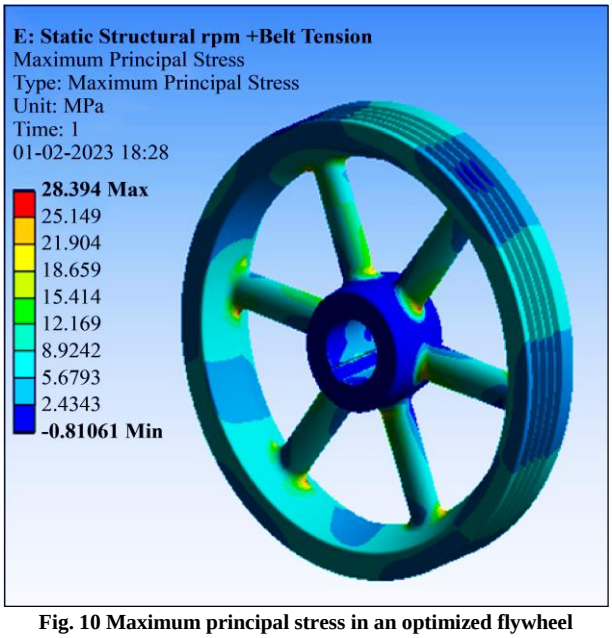

Fig. 10 Maximum principal stress in an optimized flywheel

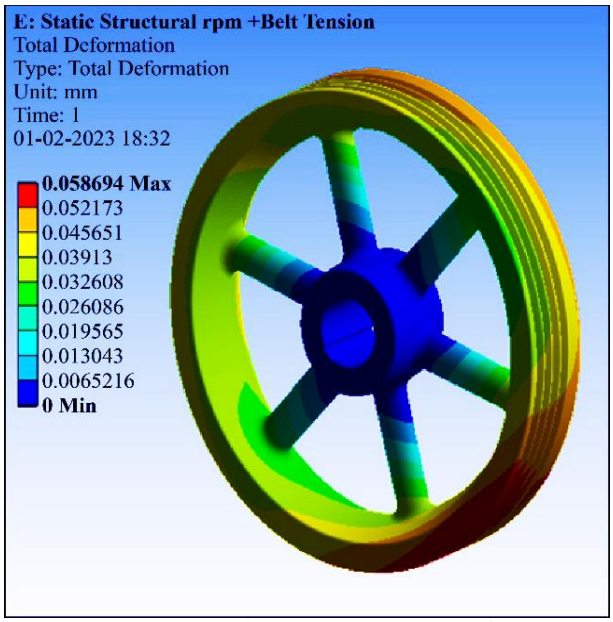

Fig. 11 Maximum deformation in an optimized flywheel

The stresses obtained from the FEA analysis of the flywheel are found to be less than the permissible value. Also, the deformation was found to be within permissible limits, and it can sustain the stresses acting on the flywheel periphery.

4. Conclusion

The paper explains the single-objective optimization problem for the ideal flywheel shape. The minimization of the weight is stated in a formulation for a single objective optimization problem. The design variables are defined by the dimensions of different features of the flywheel. The mayfly algorithm is used to solve the formulized optimization problem. It is observed that a mass reduction of about 25% is obtained when the optimization is carried out in the axial direction—the stress in the flywheel increase with a reduction in weight by some amount.

Nonetheless, it can operate without any failure at the stated condition. The stresses in previous and optimized flywheel geometry are 25.802 MPa and 28.394 MPa, respectively, less than the allowable stress (28.89MPa). Thus the designer can use this optimization technique according to the objectives of the problem.

Acknowledgments

We sincerely appreciate the support provided by the project's sponsor, the Kirloskar Pneumatic Company Limited of Pune, India, as well as the guidance and support provided by Professors Dr. D.P. Hujare and O.K. Kulkarni of the MIT-World Peace University.

References

[1] Skid Mounted Water Cooled Reciprocating Compressor Design Manual, Kirloskar Pneumatic Compressor Limited.

[2] M. Elhaj et al., "Numerical Simulation and Experimental Study of a Two-Stage Reciprocating Compressor for Condition Monitoring," *Mechanical Systems and Signal Processing*, vol. 22, no. 2, pp. 374-389, 2008. [CrossRef] [Google Scholar] [Publisher Link]

[3] Trupti Bhoskar et al., "Genetic Algorithm and its Applications to Mechanical Engineering: A Review," *Material Proceedings*, vol. 2, no. 4-5, pp. 2624-2630, 2015. [CrossRef] [Google Scholar] [Publisher Link]

[4] J. Kennedy, and R. Eberhart, "Particle Swarm Optimization," *Proceedings of IEEE International Conference on Neural Networks*, pp. 1942–1948, 1995. [CrossRef] [Google Scholar] [Publisher Link]

[5] Janez Brest, Mirjam Sepesy Maučec, and Borko Bošković, "Differential Evolution Algorithm for Single Objective Bound-Constrained Optimization: Algorithm j2020," *IEEE Congress on Evolutionary Computation*, pp. 1-8, 2020. [CrossRef] [Google Scholar] [Publisher Link]

[6] Şaban Öztürk, Rehan Ahmad, and Nadeem Akhtar, "Variants of Artificial Bee Colony Algorithm and Its Applications in Medical Image Processing," *Applied Soft Computing*, vol. 97, 2020. [CrossRef] [Google Scholar] [Publisher Link]

[7] Omkar Kulkarni et al., "Ant Colony Optimization and Its Applications in Mechanical Engineering Review," *Industrial Engineering Journal*, vol. 9, no. 2, 2016. [Google Scholar]

[8] A.S. Joshi OmkarKulkarni, G.M. Kakandikar, and V.M. Nandedkar, "Cuckoo Search Optimization- A Review," *Materials Today: Proceedings*, vol. 4, no. 8, pp. 7262-7269, 2017. [CrossRef] [Google Scholar] [Publisher Link]

[9] Logeswaran Thangamuthu et al., "Design and Development of Extract Maximum Power from Single-Double Diode PV Model for Different Environmental Condition Using BAT Optimization Algorithm," *Journal of Intelligent & Fuzzy Systems*, vol. 43, no. 1, pp. 1091-1102, 2022. [CrossRef] [Google Scholar] [Publisher Link]

[10] Shashank Gurnule, and Ritesh Banpurkar, "Design, Modification & Analysis of Industrial Air Compressor (Type: VT4)," *SSRG International Journal of Mechanical Engineering*, vol. 5, no. 5, pp. 12-18, 2018. [CrossRef] [Publisher Link]

[11] Seyedali Mirjalili, Seyed Mohammad Mirjalili, and Andrew Lewis, "Grey Wolf Optimizer," *Advances in Engineering Software*, vol. 69, pp. 46-61, 2014. [CrossRef] [Google Scholar] [Publisher Link]

[12] Omkar S Bhosale, Deepak Huajre, and Murtaza S Laila, "Optimization for Squeak and Rattle Reduction using Vibration Analysis of Passenger Car Door Trim," *Noise & Vibration Worldwide*, vol. 53, no, 9-10, pp. 428-432, 2022. [CrossRef] [Google Scholar] [Publisher Link]

[13] Prem Singh, and Himanshu Chaudhary, "Optimal Shape Synthesis of a Metallic Flywheel using Non-Dominated Sorting Jaya Algorithm," *Soft Computing*, vol. 24, pp. 6623-6634, 2020. [CrossRef] [Google Scholar] [Publisher Link]

[14] Noor Fawazi et al., "Design Optimization of a Rotating Flywheel under High Centrifugal Forces using Response Surface Method," *IOP Conference Series: Materials Science and Engineering*, vol. 507, 2018. [CrossRef] [Google Scholar] [Publisher Link]

[15] Zheng-Ming Gao et al., "The Improved Mayfly Optimization Algorithm," *Journal of Physics: Conference Series*, vol. 1684, 2020. [CrossRef] [Google Scholar] [Publisher Link]

[16] L. Jiang, and C. W. Wu, "Topology Optimization of Energy Storage Flywheel," *Structural and Multidisciplinary Optimization*, vol. 55, pp. 1917-1925, 2017. [CrossRef] [Google Scholar] [Publisher Link]

[17] L. Pedrolli et al., "Shape Optimization of a Metallic Flywheel using an Evolutive System Method: Design of an Asymmetric Shape for Mechanical Interface," *Proceedings of the Institution of Mechanical Engineers, Part C: Journal of Mechanical Engineering Science*, vol. 232, no. 2, pp. 217-230, 2018. [CrossRef] [Google Scholar] [Publisher Link]

[18] L.K.Lai, and Roan Van Hoa, "Flywheel Energy Storage in Electrical System Integrates Renewable Energy Sources," *SSRG International Journal of Electrical and Electronics Engineering*, vol. 7, no. 6, pp. 27-32, 2020. [CrossRef] [Publisher Link]

[19] Valdamir Chumski, *Reciprocating and Rotary Compressor*, E & F.N. Spon, 2013.

[20] IS 210: Grey Iron Castings, Bureau of Indian Standards, 2009. [Online]. Available: https://archive.org/details/gov.in.is.210.2009

[21] Deepak P Hujare, Nitesh R Girase, and Madhuri G Karnik, "Crack Detection in Shaft by Finite Element Analysis and Experimental Modal Analysis," *European Journal of Advances in Engineering and Technology*, vol. 3, no. 10, pp. 18–24, 2016. [Google Scholar] [Publisher Link]

[22] Kirloskar Pneumatic Company Limited, Reciprocating Compressor Design Manual.

[23] Konstantinos Zervoudakis, and Stelios Tsafarakis, "A Mayfly Optimization Algorithm," *Computers & Industrial Engineering*, vol. 145, 2020. [CrossRef] [Google Scholar] [Publisher Link]

[24] Karthik Nagarajan et al., "Combined Economic Emission Dispatch of Microgrid with the Incorporation of Renewable Energy Sources Using Improved Mayfly Optimization Algorithm," *Computational Intelligence and Neuroscience*, 2022. [CrossRef] [Google Scholar] [Publisher Link]

[25] Joseph E. Shigley, and Charles R. Mischke, *Standard Handbook of Machine Design*, Chapter 7, McGraw Hill, pp. 260-280, 1997.

[26] G.M. Kakandikar et al., "Optimising Fracture in Automotive Tail Cap by Firefly Algorithm," *International Journal of Swarm Intelligence*, vol. 5, no. 1, pp. 136-150, 2020. [CrossRef] [Google Scholar] [Publisher Link]

[27] L. Jiang et al., "Shape Optimization of Energy Storage Flywheel Rotor," *Structural and Multidisciplinary Optimization*, vol. 55, pp. 739-750, 2017. [CrossRef] [Google Scholar] [Publisher Link]